Published in final edited form as:
Immunity. 2013 September 19; 39(3): . doi:10.1016/j.immuni.2013.08.007.

Minimal differentiation of classical monocytes as they survey steady state tissues and transport antigen to lymph nodes

Claudia Jakubzick[1,2,3], **Emmanuel L. Gautier**[4], **Sophie L. Gibbings**[1], **Dorothy K. Sojka**[5], **Andreas Schlitzer**[7], **Theodore E. Johnson**[2], **Stoyan Ivanov**[4], **Qiaonan Duan**[8], **Shashi Bala**[4], **Tracy Condon**[2], **Nico van Rooijen**[9], **John R. Grainger**[10], **Yasmine Belkaid**[10], **Avi Ma'ayan**[8], **David W.H. Riches**[1,2], **Wayne M. Yokoyama**[5,6], **Florent Ginhoux**[7], **Peter M. Henson**[1,2], and **Gwendalyn J. Randolph**[3,4]

[1]Department of Pediatrics at National Jewish Health, Denver, CO 80206 [2]Integrated Department of Immunology, University of Colorado, Denver, CO 80206 [3]Department of Gene and Cell Medicine, Mount Sinai School of Medicine, New York, NY 10029 [4]Department of Pathology, Washington University Medical School, St. Louis, MO 63110 [5]Department of Medicine, Washington University Medical School, St. Louis, MO 63110 [6]Howard Hughes Medical Institute, Washington University Medical School, St. Louis, MO 63110 [7]Singapore Immunology Network, Singapore (SIgN), Agency for Science, Technology and Research (A*STAR), 138648 Singapore [8]Department of Pharmacology and Systems Therapeutics, Mount Sinai School of Medicine, New York, NY 10029 [9]Department of Molecular Cell Biology, Free University Medical Center, Amsterdam, 1007 The Netherlands [10]Mucosal Immunology Section, Laboratory of Parasitic Diseases, National Institute of Allergy and Infectious Diseases, NIH, Bethesda, MD 20892.

Summary

It is thought that monocytes rapidly differentiate to macrophages or dendritic cells (DCs) upon leaving blood. Here we have shown that Ly-6C$^+$ monocytes constitutively trafficked into skin, lung, and lymph nodes (LNs). Entry was unaffected in gnotobiotic mice. Monocytes in resting lung and LN had similar gene expression profiles to blood monocytes, but elevated transcripts of a limited number of genes including cyclo-oxygenase-2 (COX-2) and major histocompatibility complex class II (MHC II), induced by monocyte interaction with endothelium. Parabiosis, bromodoxyuridine (BrdU) pulse-chase analysis, and intranasal instillation of tracers indicated that instead of contributing to resident macrophages in the lung, recruited endogenous monocytes acquired antigen for carriage to draining LNs, a function redundant with DCs though differentiation to DCs did not occur. Thus, monocytes can enter steady state non-lymphoid organs and recirculate to LNs without differentiation to macrophages or DCs, revising a long-held view that monocytes become tissue-resident macrophages by default.

Correspondence: Gwendalyn J. Randolph, PhD Dept of Pathology Washington Univ. School of Medicine 660 South Euclid Ave. St. Louis, MO 63110 Phone: 314-286-2345 grandolph@path.wustl.edu.

Introduction

In the 1960's, van Furth and Cohn used labeling with [^{3}H]-thymidine to define kinetics of monocyte transit in the bloodstream. Monocytes spent at most a few days in blood and then mobilized to various tissues, including the inflamed peritoneum (van Furth and Cohn, 1968). In their view, the data indicated that monocytes continuously replenished tissue resident macrophages. The concept was supported by the relative ease at which monocytes became macrophages in culture and (van Furth and Cohn, 1968) more recent data specifically point to the Ly-6C$^+$ subset of monocytes (Wynn et al., 2013) precursors for macrophages in inflammatory settings. Beginning in the mid-1990's, arguments developed that the fate of monocytes could be diverted from becoming macrophages and redirected to that of dendritic cells DCs), if appropriate signals were encountered (Iijima et al., 2011; Leon et al., 2007; Nakano et al., 2009; Sallusto and Lanzavecchia, 1994; Serbina et al., 2003; Wakim et al., 2008). This differentiation, like the evidence for monocyte conversion to macrophages in vivo, stemmed almost entirely from scenarios involving inflammation.

After the work of Van Furth and Cohn, an alternative possibility that macrophages renewed themselves by local proliferation rather than dependence upon monocytes was presented (Coggle and Tarling, 1984; Sawyer et al., 1982). This viewpoint was difficult to reconcile with the concept of monocytes as precursors of macrophages and it failed to gain major traction without stronger evidence than existed at the time. Recently, definitive studies have been carried out on the origin of tissue resident macrophages, starting with brain macrophages (Ginhoux et al., 2010) and then extending to many other organs (Hashimoto et al., 2013; Schulz et al., 2012; Yona et al., 2013). The data clearly indicate that in most organs, resident macrophages are derived embryonically and maintain themselves in adults by self-renewal., An exception is observed in the intestine where macrophages are continuously repopulated by circulating monocytes (Zigmond and Jung, 2013).

These recent findings, therefore, alter a key aspect of the model that the field has held on the life cycle of monocytes since the 1960s and raise new questions about the biology of monocytes and whether they indeed extravasate constitutively (Wynn et al., 2013). Here, we asked if monocytes extravasate into steady state tissues. Upon finding such monocytes, we addressed their differentiation status. Our results support a revised paradigm wherein extravasated monocytes in non-inflamed tissues retain much of their monocytic character, rather than differentiating to macrophages or DCs. Even so, they survey tissue for antigens for transport to draining lymph nodes (LNs).

Results

Classical monocytes are present in resting nonlymphoid tissues and lymph nodes

CD64 (FcγR1) selectively recognizes macrophages and Mer tyrosine kinase (MerTK) is an additional macrophage-selective marker (Gautier et al., 2012; Tamoutounour et al., 2012). Not previously tested in skin, MerTK identified dermal macrophages as well, in contrast to isotype-matched control Ab (Fig. S1A). Co-staining for MerTK and CD64 marked macrophages (Fig. 1A), but excluded DCs and monocytes. Although monocytes express CD64 (Ingersoll et al., 2010), they do not express MerTK (Fig. 1B). Skin DCs were identified as remaining MerTK$^-$ CD64$^-$ cells expressing high CD11c and major histocompatibility complex class II (MHC II) molecules (Fig. 1A). Then, by gating on cells that were neither macrophages nor DCs, monocytes were identified in skin. Gating on remaining CD11b$^+$ cells revealed two populations of F4/80^{lo} cells, with low and higher side scatter (SSC) respectively, and a high SSC population lacking F4/80 (Fig. 1A). The latter were neutrophils, whereas F4/80^{lo} high-SSC cells were eosinophils (Gautier et al., 2012). The low SSC F4/80^{lo} cells were monocytes. Alternatively, gating directly on CD64$^+$ cells

after gating out MerTK$^+$ CD64$^+$ macrophages and MerTK$^-$ CD64$^-$ CD11c^{hi} MHC II$^+$ DCs was sufficient to identify tissue monocytes (Fig. 1A). All identified monocytes expressed Ly-6C and most expressed MHC II (Fig. 1A). Use of the same strategy in digested lymph node (LN) (Fig. S1B) and lung (Fig. 1C) permitted identification of monocytes in these locations. In all tissues, monocytes accounted for all low SSC, CD11b^{hi} cells with low to intermediate CD11c (Fig. 1A, C, D). Macrophages and DCs were larger and had more granular cytoplasm resulting in greater SSC than monocytes, consistent with properties expected of bona fide monocytes (Fig. 1D). The frequency of extracted monocytes was roughly equal to macrophages in nonlymphoid tissues (Fig. S2), whereas we extracted fewer macrophages from LNs than monocytes. These ratios may underestimate macrophages, notoriously challenging to extract. LN monocytes were one-tenth the frequency of total LN DCs (Fig. S2), but were similar in frequency to migratory, lymph-derived DCs in resting LNs (Jakubzick et al., 2008a). Taken together, we conclude that classical monocytes constitutively populate non-inflamed tissues, where they express MHC II.

Extravascular monocytes resemble MHC II$^+$ blood monocytes

Classical monocytes are thought to lack MHC II (Geissmann et al., 2003; Ingersoll et al., 2010). Detection of MHC II$^+$ monocytes in tissues and LNs prompted us to re-examine blood for MHC II$^+$ monocytes. A minority of monocytes were MHC II$^+$. These were high or intermediate for Ly-6C (Fig. 2A-B). Because MHC II$^+$ monocytes showed a spectrum of Ly-6C expression, it was optimal to divide monocyte subsets according to CD43 (leukosialin) expression rather than Ly-6C (Fig. 2A). CD43 differentially defines the major subsets of monocytes in all species examined to date (Ziegler-Heitbrock, 2007). Classical CD43^{lo} monocytes were divisible into three subsets: Ly-6C$^+$MHCII$^-$, Ly-6C$^+$MHCII$^+$ and Ly-6C$^-$MHCII$^+$ (Gates 1-3) with frequencies in blood among total monocytes of 36.1%, 8.9% and 1.0%, respectively (Fig. 2A-B). CD43^{hi} monocytes were divided into two subsets: Ly-6C$^-$MHCII$^-$ and Ly-6C$^-$MHCII$^+$ (Gates 4, 5) at frequencies of 41.9% and 8.1% (Fig. 2A-B) among total monocytes.

In CX$_3$CR1^{gfp} mice, where blood monocyte subsets express distinct intensities of GFP (Geissmann et al., 2003), gates 1-3 of blood CD43^{lo} monocytes displayed a graded increase in GFP intensity (Fig. 2C) that correlated positively with MHC II but inversely to Ly-6C. In CD43^{hi} monocytes (Gates 4 and 5), GFP intensity was characteristically high (Geissmann et al., 2003) regardless of MHC II (Fig. 2C). Monocytes in tissue and LNs had overlapping GFP intensity with monocytes in blood that were Ly-6C$^+$MHCII$^+$ (Gate 2) (Fig. 2D). Furthermore, in Lyz2-cre × RosaEGFP$^{flox/+}$ reporter mice, the frequency of GFP$^+$ cells differs between monocyte subset (Jakubzick et al., 2008a). Analysis of the blood for MHC II$^+$ monocytes revealed that all the CD43^{lo} monocytes (Gates 1-3), regardless of MHC II expression had a similar frequency of GFP$^+$ cells, and that all CD43^{hi} monocyte subpopulations (subsets 4 and 5) shared the same GFP$^+$ frequency (Fig. 2E), but distinct in frequency from CD43^{lo} monocytes (Fig. 2E) (Jakubzick et al., 2008a). In tissue and LNs of *Lyz2-cre* × RosaEGFP$^{flox/+}$ mice, Ly-6C$^+$MHCII$^+$ monocytes displayed similar EGFP frequency as observed for blood Ly-6C$^+$MHCII$^+$ monocytes (Gate 2) (Fig. 2F), indicating that within tissues these monocytes still resembled blood monocytes and had not induced further expression of lysozyme as observed in differentiated macrophages (Jakubzick et al., 2008a). Tissue monocytes did not likely derive from Ly-6C$^-$MHCII$^-$ monocytes (gate 4) since tissue monocytes express a lower EGFP frequency than Ly-6C$^-$MHCII$^-$ blood monocytes (Jakubzick et al., 2008a), because once EGFP is turned on within a cell, it becomes irreversibly marked, and cannot revert to an EGFP$^-$ cell.

Next, we compared gene expression profiles of monocytes with macrophages and DC populations. Upregulation of MHC II on Ly-6C$^+$ blood monocytes was accompanied by limited change in gene expression. Only 4 mRNA transcripts were ≥ 3-fold more abundant

(Fig. S3, panel A; Table S1 lists mRNA transcripts ≥ 2-fold elevated), including *Tmem176b* in the CD20 family, *Mrc1* encoding CD206 (mannose receptor), the receptor tyrosine kinase *Axl* closely related to *Mertk*, and MHC II (*H2-Aa*). By flow cytometry, CD206 was selectively detected on MHC II^+ Ly-$6C^{hi}$ monocytes (Fig. S3, panel B). No transcripts were significantly downregulated.

Our goal was to ask whether tissue monocytes were similar to blood monocytes, macrophages, or DCs, as Ly-$6C^+$$MHCII^+$ cells in inflamed tissues have been called tumor necrosis factor and inducible nitric oxide-producing (Tip) DCs or inflammatory DCs (Aldridge et al., 2009; Nakano et al., 2009; Serbina et al., 2003). Principle component analysis using data available from Immgen (http://www.immgen.org) revealed that LN monocytes clustered most closely with blood monocytes (Fig. 3A). Analyzed DCs included Langerhans cells (LC), other migratory DCs in skin-draining LNs (SLN) (Fig. 3A), and LN resident $CD4^+$ and $CD8^+$ DCs(Fig. 3A). Lymph-migratory DCs from distinct sources clustered (Miller et al., 2012), but LN monocytes did not cluster with migratory DCs or LN resident DCs, so it is more reasonable to classify LN monocytes as monocytes rather than DCs.

We extended analysis of tissue monocytes to include those in lung. As Affymetrix had updated their platform by the time we made this second round of isolations, we did not combine the new data. Instead, we reprofiled LN monocytes (from SLN or mesenteric LN, MLN), Ly-$6C^+$ blood monocytes (gate 1), and the two distinct $CD11b^-$ and $CD11b^+$ lung macrophages (Fig. 1C). Lung monocytes clustered with LN and blood monocytes more closely than with either macrophage population (Fig. 3B). A few dozen mRNA transcripts were elevated ≥ 3-fold in tissue monocytes relative to blood. Many of these transcripts were upregulated in common between lung and LN monocytes, pointing to a common signature induced upon monocyte entry into tissues (Fig. 3C, Table S2). This signature included *Ptgs2* encoding cyclo-oxygenase 2 (COX-2), *Il1b* encoding interleukin 1beta, *Tnfaip3* encoding A20, and *Itgax* encoding CD11c (Fig. 3C). CD11c was not expressed on Ly-$6C^+$ blood monocytes (Ingersoll et al., 2010) but was observed on tissue monocytes, albeit lower than on DCs (Fig. 1). Immunostaining analysis revealed COX-2 in Ly-$6C^+$ mononuclear cells in lung parenchyma (Fig. 3D), indicating expression of COX-2 in lung monocytes, along with its expression on neighboring DCs that were detected as cells expressing more MHC II in the lung than tissue monocytes (Fig. 3D). Ptgs2 mRNA is expressed by $CD11b^+$ $CD24^+$ DCs in the Immgen database, fitting with these results. Some transcripts were upregulated only in lung or LN monocytes (Table S2). Flow cytometry for chemokines (Eberlein et al., 2010) whose transcripts were upregulated only in LN but not lung monocytes, including CCL5 and CXCL10, stained LN monocytes more distinctly than lung monocytes (Fig. 3E). An interferon (IFN) signature was observed in LN but not lung monocytes (CXCL9, CXCL10, etc) (Table S2). Neutralizing IFN-γ did not reduce MHC II on blood monocytes (Fig. S4) and mice lacking IFN–γ and type I IFN receptor also retained MHC II^+ blood monocytes (unpublished observations).

Thus, tissue monocytes derived from steady state organs closely resemble blood monocytes, rather than macrophages or DCs. The persistence of monocytes as bona fide monocytes in tissues likely applies only to steady state tissues since monocytes recruited to sites of inflammation, differentiated into macrophages and clustered with macrophages resident in that organ. That is, thioglycollate-elicited monocyte-derived peritoneal macrophages (labeled as “PC Mo-MF” with MHC II (II^+) or without MHC II (II^-), Fig. 3A) clustered with resident macrophages. Perhaps monocytes that enter tissues on an ongoing steady state basis fail to differentiate to macrophages but remain similar to blood monocytes that have been activated, whereas in inflammation, they differentiate to macrophages. To evaluate this idea, we next sought more information on the tissue monocyte life cycle in the steady state.

Life cycle and fate of extravascular monocytes

We depleted blood monocytes using i.v. liposomal clodronate that nearly completely depleted blood monocytes for one day with a gradual recovery thereafter (Fig. 4A). In lung, extravascular tissue monocytes persisted for up to 3 days after monocytes were depleted (Fig. 4A). Monocyte frequency in these tissues was normalized to that of B cells, as B cells are not targeted for depletion. When we normalized to total $CD45^+$ cells or total cells recovered, similar results were obtained. In SLN, monocyte numbers also did not dip significantly for 3 days (Fig. 4B). However, in MLN, depletion of blood monocytes reduced LN monocytes by half in one day (Fig. 4B), with slow recovery in parallel with blood (Fig. 4B).

We next pulsed mice with bromodeoxyuridine (BrdU) i.p. To be sure that tissue monocytes evaluated were not mixed with blood monocytes that remained within the vasculature of tissues as they were processed, we injected anti-CD45 mAb i.v. two minutes before euthanasia. This technique was effective in skin and LNs where most typically we found no lingering blood monocytes but occasionally a minor fraction (Fig. 4C). The method was not useful in lung, resident DCs were labeled as were lung monocytes (Fig. 4C), indicating that anti-CD45 mAb readily accessed the highly vascularized lung. However, persistence of lung monocytes after i.p. injection of liposomal clodronate and the general lack of blood monocyte contamination in other tissues suggested that lung monocytes were not heavily contaminated. Tissue monocytes did not proliferate in situ; there were very few $BrdU^+$ monocytes in the various organs 2 h after BrdU was given (Fig. 4D). Peak labeling occurred in blood at 24 h when nearly half of monocytes were $BrdU^+$ (Fig. 4D). At 48 h, the frequency of $BrdU^+$ lung and MLN monocytes mirrored that of blood (Fig. 4D). These sites showed only a slight delay in $BrdU^+$ monocyte clearance (slope of line between 48 and 96 h), suggesting that the residence time for monocytes was brief, ≤ 1 day. Indeed, a rapid turnover of monocytes in the MLN was predicted from use of liposomal clodronate (Fig. 4A-B). Turnover of skin monocytes was different. Labeling of skin and SLN monocytes lagged , consistent with of the finding that monocytes in SLN were more persistent after liposomal clodronate. SLN monocytes labeled more quickly than skin monocytes, suggesting that some SLN monocytes arose from blood monocytes passing into SLN across HEV (Nakano et al., 2009). However, clearance of $BrdU^+$ monocytes was also slowest for SLN and consistent with the possibility that SLN monocytes might be in part derived from skin monocytes emigrating to the LN from skin lymphatics (Fig. 4D). The frequency of BrdU labeling in macrophages from skin and lung $CD11b^-$ or $CD11b^+$ macrophages was distinct from monocytes and consistent with a low, basal rate of proliferation that was somewhat higher in $CD11b^+$ macrophages compared with the more prominent $CD11b^-$ lung macrophage population (Fig. S5). Because by day 10, all $BrdU^+$ monocytes had entered and been cleared from each tissue, we were confident that we had identified a sufficient frame of time (10 days) to track a full tissue monocyte life cycle in skin, lung, and different LNs.

Thus, we next wondered whether some monocytes in these tissues differentiated to macrophages. Few macrophages were extracted from LNs (Fig. 1C), so we focused on macrophages in the lung, where two subpopulations are clearly evident (Fig. 1D), and on skin macrophages. Whereas the main population of lung macrophages is embryonically derived (Hashimoto et al., 2013; Yona et al., 2013), the life cycle of the $CD11b^+$ lung macrophages has not been studied in detail. We carried out parabiosis between CD45.1 and CD45.2 WT partners or WT and $Ccr2^{-/-}$ partners, where WT monocytes efficiently repopulate the $Ccr2^{-/-}$ host (Hashimoto et al., 2013), examining chimerism at 2 weeks and 1 year after parabiosis. Neither macrophage population (CD11b− or CD11b+) were replenished by circulating cells, whereas tissue monocytes between parabionts efficiently exchanged (Fig. 4E). When we separately analyzed macrophages in alveolar lavage, the

same outcome was observed. In skin, by contrast, macrophages were partially replenished by circulating precursors derived from the partner parabiont at 2 weeks (Fig. 4F, left graph) and nearly fully by 1 year (Fig. 4E, right graph), suggesting that monocytes are critical precursors for skin macrophages. We conclude that monocytes enter some organs like lung constitutively for purposes other than to replenish macrophages. Recent data also suggest they do not give rise to DCs in the lung (Satpathy et al., 2012). Thus, the life cycle of monocytes can include trafficking into tissues without obligatory differentiation to macrophages or DCs. These observations raised the question as to whether monocytes failing to become macrophages complete their life cycle as local monocytes that eventually die or whether they might move out of the tissue by emigrating to draining LNs, which we set out to test.

Monocyte trafficking to tissues is not driven by commensal bacteria

The frequency of monocytes in MLN and SLN was greater than in lung-draining mediastinal LNs (Fig. 5A). Thus, we wondered if tissues in contact with microbiota (skin and gut) recruited Ly-6C$^+$MHCII$^+$ monocytes due to mild commensal-driven inflammatory signals. However, the frequency of Ly-6C$^+$MHCII$^+$ monocytes in the LN (Fig. 5B) or skin (Fig. 5C) was similar between germ-free and conventionally housed mice. Extravascular neutrophils were also found in skin (Fig. 1A), but in contrast to monocytes, their recruitment was significantly reduced in germ-free mice (Fig. 5D). Finally, monocyte subset frequency in the blood of germ-free mice showed a greater proportion of Ly-6C$^+$ monocytes (Fig. 5E), though total monocyte numbers were not different between germ-free and conventionally housed mice, indicating that the development of Ly-6C$^-$ monocytes from Ly-6C$^+$ monocytes was at least partially regulated by microbial signals. Overall, however, the mobilization of monocytes into tissues was unaffected by the presence or absence of microbial colonization.

Monocytes use CD62L to enter nonlymphoid and lymphoid tissue and transport antigens to LNs via the lymphatic vasculature in the steady state

We next investigated the trafficking patterns of tissue monocytes and molecules involved. In *Ccr2*$^{-/-}$ mice, *Ccr2*$^{-/-}$ mice had greatly reduced monocytes in skin (Fig. 6A) and LNs (Fig. 6B). By contrast, LN Ly-6C$^+$MHCII$^+$ monocytes were elevated in *plt/plt* (mice lacking CCR7 ligands) and *Ccr7*$^{-/-}$ mice, consistent with previous studies (Nakano et al., 2009) (Fig. 6B). Monocyte frequency was unaffected in LNs and tissue of *Cx3cr1*$^{gfp/gfp}$ and *Sell*$^{-/-}$ mice (Fig. 6B). However, when chimeric mice were generated using lethally irradiated recipient mice reconstituted with a 1:1 mixture of CD45.1$^+$ WT and CD45.2$^+$ *Sell*$^{-/-}$ bone marrow (BM) cells (WT: *Sell*$^{-/-}$); CD45.1$^+$ WT and CD45.2$^+$ *Ccr7*$^{-/-}$ BM cells (WT:*Ccr7*$^{-/-}$); or CD45.1$^+$ WT and CD45.2$^+$ WT BM cells (WT:WT), *Sell*$^{-/-}$ derived monocytes selectively showed a modest disadvantage in gaining access to skin-draining LNs (Fig. 6C). A disadvantage for *Sell*$^{-/-}$ monocytes was further observed in their arrival to skin (Fig. 6D), whereas *Sell*$^{-/-}$ Ly-6C$^+$MHCII$^+$ monocytes modestly accumulated relative to WT counterparts in blood (Fig. 6E). Although CD62L encoded by *Sell* is well known for its role in mediating passage of leukocytes across HEV, it also mediates passage into skin (Leon and Ardavin, 2008). Thus, the advantage of WT derived monocytes present in the LN over *Sell*$^{-/-}$ derived monocytes may be due to a passage of monocytes across HEV from the bloodstream and also an impact on monocyte trafficking first into skin and subsequently to LNs through afferent lymphatics. To investigate the migration of undifferentiated monocytes to LNs through afferent lymphatics, we adoptively transferred purified Ly-6C$^+$MHCII$^-$, Ly-6C$^+$MHCII$^+$, or Ly-6C$^-$MHCII$^-$ blood monocytes into skin. Notably, only Ly-6C$^+$MHCII$^+$ monocytes, but not MHC II$^-$ or Ly-6C$^-$ monocytes migrated to draining LNs (Fig. 6F). In LNs, these cells had lost Ly-6C expression, seemingly different

than our observations for endogenous monocytes, but this may be due to having sorted on monocytes using Ly-6C mAb that may have stimulated internalization of surface Ly-6C.

Emigration of transferred MHC II$^+$ monocytes from skin to SLN (Fig. 6F) and data from BrdU labeling consistent with this concept (Fig. 4E) led us to wonder whether steady trafficking monocytes might survey tissues and transfer antigens to LNs, all the while retaining close resemblance to monocytes (Fig. 3). We used an experimental approach in which FITC-conjugated lipopolysaccharide (LPS)-free chicken ovalbumin (OVA) administered i.n. quantitatively tracks trafficking of DCs to LNs in the steady state (Jakubzick et al., 2008b). We asked whether monocytes also acquired FITC-OVA in the lung and transported it to the lung--draining lymph node (LLN) in the absence of inflammation, how this transport compared quantitatively to migration of DCs transporting FITC-OVA, and how inflammation in the lung affects transport of FITC-OVA by minimally undifferentiated monocytes. For these assays, we relied on previous insight that some sources of chicken OVA induce inflammation but other sources do not perturb steady state leukocyte trafficking (Jakubzick et al., 2008b). Approximately 6% of monocytes gated in LNs were FITC-OVA$^+$ at 24 h after FITC-OVA was administered i.n. (Fig. 6G), thus indicating that monocytes in the LN at least are partly sustained through lymphatic input of monocytes. Furthermore, these data show that monocytes participate in antigen surveillance in upstream peripheral tissues and emigrate with this antigen to LNs without differentiating to cells other than monocytes (such as DCs or macrophages). To get a quantitative sense as to how this basal transport compared to DCs, we quantified the ratio of FITC-OVA$^+$ DCs in the same LN as FITC-OVA$^+$ monocytes. OVA$^+$ DCs still outnumbered monocytes by ~10-fold. Nonetheless, the data indicate that monocytes have a role in basal antigen transport to the steady state LN. These monocytes may stimulate T cell responses in LNs, as we observed the stimulation of naïve OT-I transgenic T cells in vitro when blood monocytes, especially the MHC II$^+$ subset of Ly-6C$^+$ monocytes were purified, pulsed with OVA ex vivo, and cultured with T cells for 60 h (Fig. S6). When inflammation-inducing OVA was used to analyze antigen trafficking monocytes to the draining LN, the fraction of labeled monocytes approximately doubled but still left DCs dominant in overall antigen transport (Fig. 6G).

To provide an infectious context with more robust inflammation, we inoculated anthrax spores into the airway. CFSE was delivered i.n. 2 or 3 days after spore delivery. CFSE administered i.n. does not enter freely into the LNs (Jakubzick et al., 2008b). Four days after spore and CFSE delivery, CFSE$^+$ monocytes were observed in the lung-draining LN (LLN), along with MHCII^{hi} migratory DCs (Fig. S7). Here, again, DCs dominated as the main emigrating CFSE$^+$ cell type, but monocytes represented a substantial fraction of the total CFSE$^+$ migratory cells. Thus, monocytes participate in steady state tissue surveillance and antigen transport that involves homeostatic monocyte recruitment to various organs followed by emigration to LNs through lymphatic vessels. In this process, monocytes undergo only limited differentiation including the upregulation of MHC II, but still most closely resemble monocytes.

Ly-6C$^+$MHCII$^-$ monocytes in the blood are precursors for blood and tissue MHC II$^+$ monocytes

Finally, we compared the fate of Ly-6C$^+$MHCII$^-$ versus Ly-6C$^+$MHCII$^+$, or Ly-6C$^-$MHCII$^-$ blood monocytes that were isolated and sorted from CX3CR1^{gfp} mice and intravenously transferred into mice bearing congenic CD45, thus providing two criteria for subsequent identification of rare transferred cells--GFP and congenic CD45 alleles. Immediately after monocyte transfer, recipient mice were given injection of 2 μg of LPS intradermally (i.d.) to enhance the attraction of grafted monocytes to skin. In the blood, a minority of Ly-6C$^+$MHCII$^-$ monocytes had converted to Ly-6C$^+$MHCII$^+$ monocytes (Fig.

7A), whereas the transferred Ly-6C$^+$MHCII$^+$ monocytes or Ly-6C$^-$MHCII$^-$ monocytes had scarcely changed from their phenotype at original sorting, although some of the transferred Ly-6C$^+$MHCII$^+$ monocytes had lost Ly-6C expression (Fig. 7A).

Ly-6C$^-$ monocytes failed to enter SLNs (Fig. 7B), but transferred Ly-6C$^+$MHCII$^-$ blood monocytes and their separately sorted blood MHC II$^+$ counterparts entered. Such monocytes were MHC II$^+$ and Ly-6C$^+$, whereas transferred Ly-6C$^+$MHCII$^+$ monocytes had lost Ly-6C (Fig. 7B). Thus, entry into the LN is not restricted to MHC II$^+$ blood monocytes. Transferred cells were difficult to retrieve from the skin, but those that were retrieved from transfer of Ly-6C$^+$MHCII$^-$ monocytes also showed induction of MHC II following, or in concert with, their arrival in the skin (Fig. 7C), whereas Ly-6C$^-$ monocytes did not enter skin (Fig. 7C). Taken together, these transfer data suggest that Ly-6C$^+$MHCII$^-$ are the precursors for blood and tissue Ly-6C$^+$MHCII$^+$ monocytes therein.

That Ly-6C$^+$MHCII$^-$ monocytes upregulated MHC II after their arrival in skin or SLN (Fig. 7A-C) seemed at odds with the finding that injecting these cells directly into skin did not lead to their ability to migrate to LNs, since MHC II$^+$ monocytes were able to mobilize to LNs (Fig. 6). Since emigration and MHC II expression are known to be coupled (Faure-Andre et al., 2008), we wondered if direct injection of Ly-6C$^+$MHCII$^-$ monocytes in the skin might be associated with a failure of the monocytes to upregulate MHC II. Indeed, Ly-6C$^+$MHCII$^-$ monocytes purified from the blood and injected into skin for retrieval 18 h later did not upregulate MHC II (Fig. 7D), in contrast to their ability to do so if re-injected in the blood (Fig. 7C), raising the possibility that conversion of Ly-6C$^+$MHCII$^-$ monocytes to Ly-6C$^+$MHCII$^+$ monocytes requires migration through or interaction with the endothelium. In support of this possibility, mouse Ly-6C$^+$MHCII$^-$ monocytes cultured with endothelial cells, but not fibroblasts, supported a robust upregulation of MHC II (Fig. 7E). Thus, the appearance of classical monocytes expressing MHC II in tissues arises from the recruitment of MHC II$^-$ rather than MHC II$^+$ monocytes from blood and the induction of MHC II may be stimulated by transendothelial migration. These monocytes in turn have the ability to survey for antigens in the tissue and emigrate to lymph nodes, all the while remaining as monocytes, rather than differentiating to macrophages or DCs.

DISCUSSION

Compelling analysis of lineage indicates that most, if not all, organs contain a population of macrophages derived not from monocytes but from embryonic macrophage progenitors that develop in the embryo before definitive hematopoiesis occurs (Hashimoto et al., 2013; Schulz et al., 2012; Yona et al., 2013). Schulz et al. further concluded that all fetal organs contained a second macrophage pool that was of bone marrow origin. The nature of this second macrophage pool was minimally characterized, but was defined as a population with lower F4/80, expression of MHC II, CCR2, and CD11b. Our data indicate that this second pool in organs like lung are not macrophages but rather monocytes that do not contribute to the resident macrophage pool. By contrast, skin macrophages, like intestinal macrophages (Zigmond and Jung, 2013), appear to deriveat least partly from monocytes.

The pool of monocytes constitutively entering tissues is not the subset earlier claimed to constitutively traffic into tissues from blood (Geissmann et al., 2003), as we did not identify Ly-6C$^-$CD43^{hi} monocytes in extravascular tissues, but instead classical Ly-6C$^+$ monocytes. Indeed, the concept that resident tissue macrophages are seeded prior to birth raises new questions about the biology of monocytes in the absence of infection or sterile inflammation. Wynn et al. have raised this question and suggested that monocytes may not enter tissues constitutively, assuming that the raison d'être for doing so no longer applied with the revelation that macrophages derive embryonically (Wynn et al., 2013). We have shown they

do, but not because they are obliged to differentiate to macrophages or DC following diapedesis. They come into tissues, a step partially dependent upon CD62L, at least in part to survey the environment and then emigrate to LNs, and they are able to do this with only minimal differentiation, such that we are left to best classify them simply as tissue monocytes.

Ly-6C^{+}MHCII^{+} monocyte-derived or monocyte-like cells have been given many different names in the literature, including myeloid-derived suppressor cells (Ochando and Chen, 2012), Tip-DCs (Aldridge et al., 2009; Serbina et al., 2003), inflammatory DCs (Nakano et al., 2009), inflammatory monocytes (Soudja et al., 2012), and effector monocytes (Leiriao et al., 2012). Typically in these scenarios when they are studied for their role in antigen presentation it is in the context of inflammatory reactions (Iijima et al.; Leon et al., 2007; Nakano et al., 2009; Serbina et al., 2003; Soudja et al., 2012; Wakim et al., 2008). In LNs, they have been argued to enter through the HEV (Nakano et al., 2009), with no information on how, after entering via such a route that they would gain access to the antigen they appear to present. Soluble antigen is largely sequestered in LN conduits, and it appears that sampling of antigen from conduits alone is insufficient to drive a productive immune response (Itano et al., 2003). In agreement with Ardavin and colleagues (Leiriao et al., 2012), we have shown here that monocytes retaining features of minimally differentiated monocytes transport molecules from the nonlymphoid tissues to draining LNs, but we have extended this observation to showing its occurrence in the steady state, with all the while the cells retaining surface and gene expression profiles of monocytes. Consistent with this concept, studies in rat lymph have identified monocytes in resting lymph (Yrlid et al., 2006), but largely ignored them while focusing on the smaller fraction of those that could be called bona fide DCs.

Therefore monocytes appear to share with DCs the characteristic of tissue surveillance even without becoming DCs. However, the effector mechanisms used by DCs and monocytes need not be the same. Monocytes may support antigen presentation and adaptive immunity by means that do not require they act as the antigen-presenting cell per se. Indeed, when directly analyzed, monocytes displaying Ly-6C, MHC II, and CD11c, perhaps similar to the cells studied here, are poor presenters of antigen (Drutman et al., 2012) and alternative mechanisms have been identified as to how monocytes potently support adaptive immunity (Soudja et al., 2012). Thus, we believe the literature, when combined with our findings, supports a model of the monocyte as a surveillance and effector cell in tissues that is complementary to but does not necessarily duplicate the role of lymph-homing DCs.

Although this work suggests that constitutively trafficking monocytes are not obliged to fully differentiate to macrophages or DCs after they enter tissues, we underscore that monocytes can differentiate to macrophages. Thioglycollate-elicited monocytes,which rapidly lose Ly-6C expression after emigrating from the blood, cluster not with monocytes as do Ly-6C^{+} extravascular monocytes but with resident peritoneal macrophages and they upregulate the genes universally associated with macrophages (Gautier et al., 2012). It seems from our data that differentiation to macrophages is not obligatory following monocyte entry, and triggers may be necessary to drive such differentiation. Indeed, the organs wherein macrophages are derived from monocytes in the steady state—skin and intestine—are those that receive stimulation from microbiota continuously. Although infiltration of skin by monocytes was not reduced in germ-free mouse colonies, future studies will be needed to address whether the differentiation of monocytes to macrophages in skin does depend upon microbial stimuli.

The retention of Ly-6C expression in extravascular monocytes may be a convenient signature of cells retaining monocyte status in extravascular tissues. While more profiling

will be needed to establish Ly-6C as such a transitional marker, it is very interesting that recent work in the intestine has tracked the fate of monocytes in different disease scenarios using Ly-6C, MHC II, and CD64 expression. In this case, in highly inflammatory scenarios (e.g., colonic inflammation, Crohn's disease), monocytes fail to differentiate beyond the Ly-6C^{+}MHCII^{+} stage, whereas in healthy colon they fully downregulate Ly-6C and become IL-10-producing macrophages (Bain et al., 2013; Tamoutounour et al., 2012).

Gene expression profiles were not identical between blood and extravascular LN monocytes, though they were similar. Prominent among upregulated genes was a common signature between the two tissue monocytes—those from lung and SLN—that we were able to sort in sufficiently large numbers. This included upregulation of mRNA transcripts that are often associated with inflammation and inflammasome or cytokine receptor activation, and transcripts often associated with DCs (CD11c, MHC II, CD83). The mRNA transcript encoding COX-2 (*Ptgr2*), known to be an activation-induced transcript, was expressed in situ, arguing that the common tissue monocyte signature was not a result of activation during isolation and flow cytometric cell sorting. COX-2 has been associated with the monocyte-derived cell's ability to produce PGE2 during infection with Toxoplasma gondii (Grainger et al., 2013). Such production protects the host against neutrophil-mediated damage (Grainger et al., 2013) and maintenance of tissue integrity. The emergence of COX-2 in the common tissue monocyte signature might suggest that tissue monocytes fulfill this same role, albeit at lower magnitude, in the steady state.

In conclusion, we have identified an extravascular population of classical monocytes in resting tissues that in some organs may account forthe previously proposed second population of tissue macrophages (Schulz et al., 2012). Studies in various reporter mice and gene expression profiling support the concept that in naïve tissues, extravascular monocytes differentiate only minimally in the steady state and do not become bona fide macrophages by molecular criteria. Considering that the major populations of resident macrophages do not rely on monocytes as precursors, our data compel us to propose that monocytes be viewed not just as precursors for either macrophages or DCs but as mononuclear phagocytes with functions and roles in their own right—cells with the option, but not the obligation, to differentiate to macrophages in response to cues that remain to be defined.

MATERIALS AND METHODS

Mice and treatments

C57BL/6 mice were used at 6–8 wk of age using protocols approved by Mount Sinai School of Medicine, University of Colorado, NIAID, or Washington University. Strains were from Jackson Laboratory, except germ-free (GF) mice were bred at the Washington University Digestive Diseases Core Center or maintained in isolators at the NIAID gnotobiotic facility. Parabiosis was carried out as described (Hashimoto et al., 2013). For BrdU labeling, mice were injected with 1 mg of BrdU (Life Technologies Corporation) i.p. and then euthanized at the indicated time points. BrdU incorporation into DNA was detected using the BrdU Staining Kit (eBiosciences).

Tissue Preparation, Flow Cytometry

Perfused tissues were minced. Lung and LNs were digested using 2.5 mg/ml collagenase D (Roche) for 30 min at 37°C. Skin was digested in RPMI 1640 plus 1.75mg/ml Liberase TM (Roche) at 37°C for 25 min. These mAbs and isotype-matched control mAbs purchased from Biolegend were used for flow cytometry staining: Pacific blue–conjugated mAbs to I-A and I-E or Gr1; PE-conjugated mAbs to CD115, Siglec F, CD11b, CD8, CD103, or I-A and I-E; PerCP-Cy5.5–conjugated mAbs to Ly-6C, CD11b; PE-Cy7–conjugated mAb to

CD43, CD11c; allophycocyanin-conjugated mAbs to Ly-6C, CD93, CD103, Gr1, CD64 or I-A and I-E; and allophycocyaninCy7-conjugated mAbs to B220, NK1.1; FITC-conjugated mAbs to CD43 or CD36. F480-FITC was purchased from Serotec. Anti-MerTK was from R&D Systems. Chemokine expression was analyzed as described (Eberlein et al., 2010).

As part of ImmGen, for cell sorting, we followed procedures are outlined in extensive detail at http://www.immgen.org. Briefly, to sort blood monocytes, staining for CD115, CD43, Ly-6C– MHC II was done to identify monocyte subsets. FSC-W and dump-channel staining for NK1.1, CD3, and B220 were used to improve purity. Lung and LN monocytes were stained similarly but with MerTK, CD64, F4/80 and CD11b instead of CD115, which is lost after collagenase digestion. Lung or LNs were digested in Collagenase D (Roche) for 30 min at 37° C and cells were stained with conjugated mAbs. 15-20 mice.. Blood was collected by cardiac puncture and red blood cells were lysedand remaining leukocytes stained for cell sorting. All cells sorted were $B220^{-}$ and $NK1.1^{-}$ to exclude B cells and NK cells that readily attach to monocytes. Propidium iodide excluded dead cells. The entire procedure from the time mice were euthanized to direct collection of cells after the second sort in TRIZOL was < 3 h.

Immunostaining

Immunostaining of tissue sections was carried out using appropriate isotype-matched controls or biotinylated anti-Ly-6C mAb and I-A and I-E mAbs from Biolegend, along with anti-COX-2 mAb (clone 33) from Sigma.

Bone marrow transplants

Eight-week mice F1 for CD45.1 and CD45.2 congenic alleles were lethally irradiated with two doses of 650 rad 18 hours apart. After the second irradiation, recipient mice received 5×10^6 donor bone marrow cells i.v. comprised of 1:1 mixtures of the following genotypes: WT CD45.1:WT CD45.2, WT CD45.1:$CD62L^{-/-}$ CD45.2, or WT CD45.1:$CCR7^{-/-}$ CD45.2 mice. Mice were studied 8 weeks later.

Microarray analysis, normalization, and dataset analysis

Whole-mouse genome Affymetrix gene arrays were performed with the ImmGen. RNA was amplified and hybridized on Gene Chip Mouse 1.0 ST Arrays (for datasets in Figs. 3A and S3) or Gene Chip Mouse 2.0 ST Arrays (for datasets in Fig. 3B-C). Raw data were normalized using the robust multi-array algorithm. A common threshold for positive expression at 95% confidence across the dataset was determined to be 120. Differentially expressed probesets between populations were selected using a Student's T-test with Bonferroni correction ($p < 0.05$ and 2-fold change). Signature transcripts were visualized using the “Heat Map Viewer” module of GenePattern (http://www.broadinstitute.org/cancer/software/genepattern/). Pathway enrichment signatures was identified using List2Network software (http://amp.pharm.mssm.edu/lachmann/upload/register.php). Principal component analysis (PCA) was conducted using MATLAB using RMA normalized and log2 transformed expression data. Datasets were deposited at National Center for Biotechnology Information/Gene Expression Omnibus under accession number GSE15907.

Monocyte-endothelial cell interactions

Ly-$6C^{+}MHCII^{-}$ monocytes were isolated from $CX_3CR1^{gfp/gfp}$ spleens via negative selection with anti-CD3, anti-B220, anti-MHCII, anti-CD11c, anti Ly6G and anti-siglec F magnetic beads (Miltenyi). Analysis of monocyte purity was performed using flow cytometry analysis. A bovine type-1 collagen (Advanced Biomatrix) bed was prepared in microplates.Bend.3 endothelial cells, kindly provided by Jordan Jacobelli at National Jewish

Health, were placed atop the collagen to achieve confluency. 1×10^6 enriched monocytes were added to endothelial-collagen wells and co-cultured for 18 h at 37°C. Monocytes were retrieved by adding collagenase D to digest the collagen before staining and flow cytometry analysis with gating on monocytes. Control wells used 3T3 and primary lung fibroblasts instead of endothelium

Statistics

Statistical analysis using one-way ANOVA or two-tailed Student's *t* test was conducted using InStat and Prism software (GraphPad Software). All results are expressed as mean ± SEM. A value of $P < 0.05$ was considered significant.

Supplementary Material

Refer to Web version on PubMed Central for supplementary material.

Acknowledgments

We thank Christophe Benoist and the Immunological Genome Consortium (Immgen) for their roles in the gene expression analysis. We thank Jeremiah Faith and Jeffrey Gordon for gnotobiotic mice, Robert Schreiber for anti-IFNγ mAb H22, Liping Yang for technical assistance and advice with parabiosis, and Dirk Homann for assistance and reagents used in chemokine staining.. This work was supported by NIH grant AI049653 to GJR with a Primary Caregiver's Supplement to CJ. CJ and PMH were supported by NHLBI-HL81151 and NHLBI-HL115334. DWHR and TC were supported by the U.S. Department of Defense grant DOD W81XWH-07-1-0550-Mason. ELG was funded in part by the AHA (10POST4160140). DKS is supported by Training in Cancer Biology grant T32CA009547. AS and FG were supported by a Singapore Immunology Network core grant. The Immunological Genome project is funded by R24 AI072073 to C. Benoist. Funding related to the use of gnotobiotic mice was through Washington University Digestive Diseases Research Core Center (DDRCC) grant DK052574.

REFERENCES

Aldridge JR Jr. Moseley CE, Boltz DA, Negovetich NJ, Reynolds C, Franks J, Brown SA, Doherty PC, Webster RG, Thomas PG. TNF/iNOS-producing dendritic cells are the necessary evil of lethal influenza virus infection. Proc Natl Acad Sci U S A. 2009; 106:5306–5311. [PubMed: 19279209]

Bain CC, Scott CL, Uronen-Hansson H, Gudjonsson S, Jansson O, Grip O, Guilliams M, Malissen B, Agace WW, Mowat AM. Resident and pro-inflammatory macrophages in the colon represent alternative context-dependent fates of the same Ly6C(hi) monocyte precursors. Mucosal Immunol. 2013

Coggle JE, Tarling JD. The proliferation kinetics of pulmonary alveolar macrophages. J Leukoc Biol. 1984; 35:317–327. [PubMed: 6584524]

Drutman SB, Kendall JC, Trombetta ES. Inflammatory spleen monocytes can upregulate CD11c expression without converting into dendritic cells. J Immunol. 2012; 188:3603–3610. [PubMed: 22442444]

Eberlein J, Nguyen TT, Victorino F, Golden-Mason L, Rosen HR, Homann D. Comprehensive assessment of chemokine expression profiles by flow cytometry. J Clin Invest. 2010; 120:907–923. [PubMed: 20197626]

Faure-Andre G, Vargas P, Yuseff MI, Heuze M, Diaz J, Lankar D, Steri V, Manry J, Hugues S, Vascotto F, et al. Regulation of dendritic cell migration by CD74, the MHC class II-associated invariant chain. Science. 2008; 322:1705–1710. [PubMed: 19074353]

Gautier EL, Shay T, Miller J, Greter M, Jakubzick C, Ivanov S, Helft J, Chow A, Elpek KG, Gordonov S, et al. Gene-expression profiles and transcriptional regulatory pathways that underlie the identity and diversity of mouse tissue macrophages. Nat Immunol. 2012; 13:1118–1128. [PubMed: 23023392]

Geissmann F, Jung S, Littman DR. Blood monocytes consist of two principal subsets with distinct migratory properties. Immunity. 2003; 19:71–82. [PubMed: 12871640]

Ginhoux F, Greter M, Leboeuf M, Nandi S, See P, Gokhan S, Mehler MF, Conway SJ, Ng LG, Stanley ER, et al. Fate mapping analysis reveals that adult microglia derive from primitive macrophages. Science. 2010; 330:841–845. [PubMed: 20966214]

Grainger JR, Wohlfert EA, Fuss IJ, Bouladoux N, Askenase MH, Legrand F, Koo LY, Brenchley JM, Fraser ID, Belkaid Y. Inflammatory monocytes regulate pathologic responses to commensals during acute gastrointestinal infection. Nat Med. 2013; 19:713–721. [PubMed: 23708291]

Hashimoto D, Chow A, Noizat C, Teo P, Beasley MB, Leboeuf M, Becker CD, See P, Price J, Lucas D, et al. Tissue-Resident Macrophages Self-Maintain Locally throughout Adult Life with Minimal Contribution from Circulating Monocytes. Immunity. 2013; 38:792–804. [PubMed: 23601688]

Iijima N, Mattei LM, Iwasaki A. Recruited inflammatory monocytes stimulate antiviral Th1 immunity in infected tissue. Proc Natl Acad Sci U S A. 2011; 108:284–289. [PubMed: 21173243]

Ingersoll MA, Spanbroek R, Lottaz C, Gautier EL, Frankenberger M, Hoffmann R, Lang R, Haniffa M, Collin M, Tacke F, et al. Comparison of gene expression profiles between human and mouse monocyte subsets. Blood. 2010; 115:e10–19. [PubMed: 19965649]

Itano AA, McSorley SJ, Reinhardt RL, Ehst BD, Ingulli E, Rudensky AY, Jenkins MK. Distinct dendritic cell populations sequentially present antigen to CD4 T cells and stimulate different aspects of cell-mediated immunity. Immunity. 2003; 19:47–57. [PubMed: 12871638]

Jakubzick C, Bogunovic M, Bonito AJ, Kuan EL, Merad M, Randolph GJ. Lymph-migrating, tissue-derived dendritic cells are minor constituents within steady-state lymph nodes. J Exp Med. 2008a; 205:2839–2850. [PubMed: 18981237]

Jakubzick C, Helft J, Kaplan TJ, Randolph GJ. Optimization of methods to study pulmonary dendritic cell migration reveals distinct capacities of DC subsets to acquire soluble versus particulate antigen. J Immunol Methods. 2008b; 337:121–131. [PubMed: 18662693]

Leiriao P, del Fresno C, Ardavin C. Monocytes as effector cells: activated Ly-6C(high) mouse monocytes migrate to the lymph nodes through the lymph and cross-present antigens to CD8+ T cells. Eur J Immunol. 2012; 42:2042–2051. [PubMed: 22585535]

Leon B, Ardavin C. Monocyte migration to inflamed skin and lymph nodes is differentially controlled by L-selectin and PSGL-1. Blood. 2008; 111:3126–3130. [PubMed: 18184867]

Leon B, Lopez-Bravo M, Ardavin C. Monocyte-derived dendritic cells formed at the infection site control the induction of protective T helper 1 responses against Leishmania. Immunity. 2007; 26:519–531. [PubMed: 17412618]

Miller JC, Brown BD, Shay T, Gautier EL, Jojic V, Cohain A, Pandey G, Leboeuf M, Elpek KG, Helft J, et al. Deciphering the transcriptional network of the dendritic cell lineage. Nat Immunol. 2012; 13:888–899. [PubMed: 22797772]

Nakano H, Lin KL, Yanagita M, Charbonneau C, Cook DN, Kakiuchi T, Gunn MD. Blood-derived inflammatory dendritic cells in lymph nodes stimulate acute T helper type 1 immune responses. Nat Immunol. 2009; 10:394–402. [PubMed: 19252492]

Ochando JC, Chen SH. Myeloid-derived suppressor cells in transplantation and cancer. Immunol Res. 2012

Sallusto F, Lanzavecchia A. Efficient presentation of soluble antigen by cultured human dendritic cells is maintained by granulocyte/macrophage colony-stimulating factor plus interleukin 4 and downregulated by tumor necrosis factor alpha. J Exp Med. 1994; 179:1109–1118. [PubMed: 8145033]

Satpathy AT, Kc W, Albring JC, Edelson BT, Kretzer NM, Bhattacharya D, Murphy TL, Murphy KM. Zbtb46 expression distinguishes classical dendritic cells and their committed progenitors from other immune lineages. J Exp Med. 2012; 209:1135–1152. [PubMed: 22615127]

Sawyer RT, Strausbauch PH, Volkman A. Resident macrophage proliferation in mice depleted of blood monocytes by strontium-89. Lab Invest. 1982; 46:165–170. [PubMed: 6174824]

Schulz C, Gomez Perdiguero E, Chorro L, Szabo-Rogers H, Cagnard N, Kierdorf K, Prinz M, Wu B, Jacobsen SE, Pollard JW, et al. A lineage of myeloid cells independent of Myb and hematopoietic stem cells. Science. 2012; 336:86–90. [PubMed: 22442384]

Serbina NV, Salazar-Mather TP, Biron CA, Kuziel WA, Pamer EG. TNF/iNOS-producing dendritic cells mediate innate immune defense against bacterial infection. Immunity. 2003; 19:59–70. [PubMed: 12871639]

Soudja SM, Ruiz AL, Marie JC, Lauvau G. Inflammatory Monocytes Activate Memory CD8(+) T and Innate NK Lymphocytes Independent of Cognate Antigen during Microbial Pathogen Invasion. Immunity. 2012; 37:549–562. [PubMed: 22940097]

Tamoutounour S, Henri S, Lelouard H, de Bovis B, de Haar C, van der Woude CJ, Woltman AM, Reyal Y, Bonnet D, Sichien D, et al. CD64 distinguishes macrophages from dendritic cells in the gut and reveals the Th1-inducing role of mesenteric lymph node macrophages during colitis. Eur J Immunol. 2012; 42(3150):66.

van Furth R, Cohn ZA. The origin and kinetics of mononuclear phagocytes. J Exp Med. 1968; 128:415–435. [PubMed: 5666958]

Wakim LM, Waithman J, van Rooijen N, Heath WR, Carbone FR. Dendritic cell-induced memory T cell activation in nonlymphoid tissues. Science. 2008; 319:198–202. [PubMed: 18187654]

Wynn TA, Chawla A, Pollard JW. Macrophage biology in development, homeostasis and disease. Nature. 2013; 496:445–455. [PubMed: 23619691]

Yona S, Kim KW, Wolf Y, Mildner A, Varol D, Breker M, Strauss-Ayali D, Viukov S, Guilliams M, Misharin A, et al. Fate mapping reveals origins and dynamics of monocytes and tissue macrophages under homeostasis. Immunity. 2013; 38:79–91. [PubMed: 23273845]

Yrlid U, Jenkins CD, MacPherson GG. Relationships between distinct blood monocyte subsets and migrating intestinal lymph dendritic cells in vivo under steady state conditions. J Immunol. 2006; 176:4155–4162. [PubMed: 16547252]

Ziegler-Heitbrock L. The CD14+ CD16+ blood monocytes: their role in infection and inflammation. J Leukoc Biol. 2007; 81:584–592. [PubMed: 17135573]

Zigmond E, Jung S. Intestinal macrophages: well educated exceptions from the rule. Trends Immunol. 2013; 34:162–168. [PubMed: 23477922]

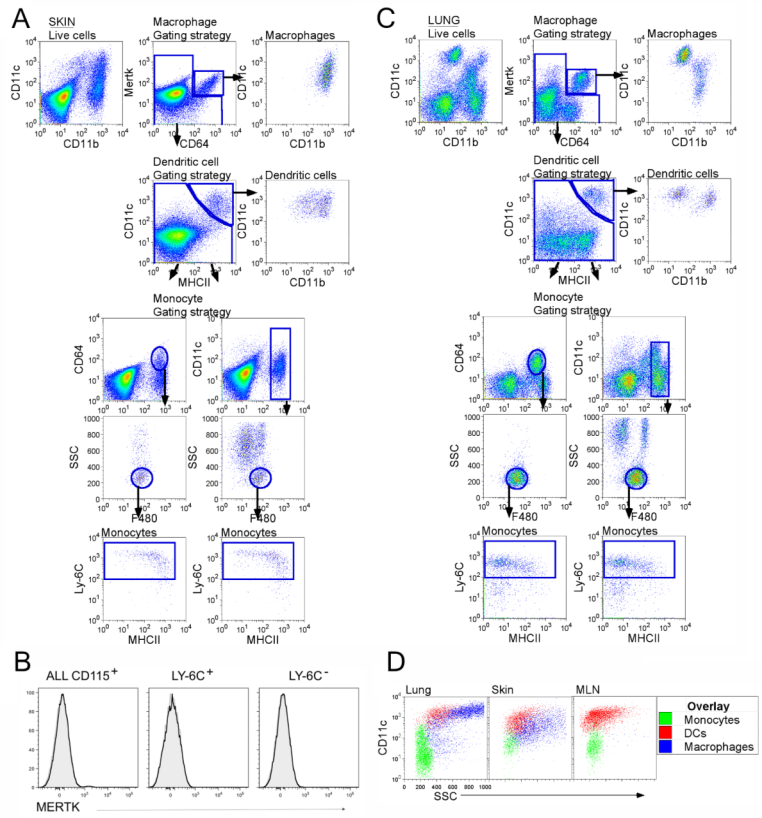

Figure 1. Analysis of tissues for the presence of monocytes

For skin (A) and lung (C), doublet-cell excluded, live cells were plotted as CD11c vs CD11b or MerTK vs CD64. Live cells plotted as MerTK vs CD64 defined tissue macrophages as MerTK^{+}CD64^{+}. Gated MerTK^{+}CD64^{+} macrophages were CD11c^{+} and CD11b^{+} (top panels). Continuing with the remaining MerTK^{-} CD64^{-} gate, DCs were identified as MerTK^{-}CD64^{-}CD11c^{+}MHCII^{+} (second row panels), with both CD11b^{hi} and CD11b^{lo} subsets. Events captured neither in the macrophage or DC gate were then plotted to depict CD64 vs CD11b or CD11c vs CD11b, allowing us to identify monocytes and granulocytes (third row panels). Tissue monocytes were low SSC F480^{+}Ly-6C^{+}MHCII^{+} (fourth and fifth row panels). B) Blood monocytes were stained with anti-MerTK mAb, but lacked reactivity. Black line, anti-Mertk mAb; gray profile, Isotype control mAb. D) SSC overlay of tissue and LN monocytes, DCs and macrophages from gates shown in A, C. Data are representative of ≥ 3 experiments. Fig. S1 accompanies this figure.

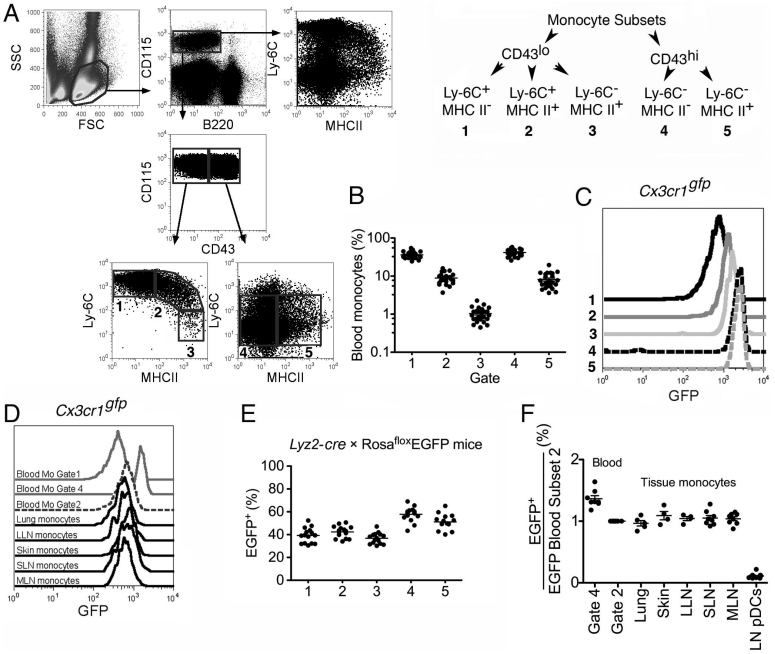

Figure 2. Analysis of blood and tissue monocytes in CX3CR1^{gfp} mice and Lyz2-cre × Rosa26 EGFP reporter mice

A) The gating strategy leading to generation of 5 gates for monocyte subsets is shown using dots plots (left) and a diagram (right). B) The frequency of blood monocyte subsets in gates 1-5 from Panel A are plotted on a log scale. C) GFP intensity of blood monocyte subsets, gates 1-5, from *Cx3cr1*$^{gfp/gfp}$ mice. D) Overlay of GFP intensity in monocytes from blood, lung, skin, and LNs in *Cx3cr1*$^{gfp/gfp}$ mice. Ly-6C^{+}MHCII$^{−}$ (gate 1) and Ly-6C$^{−}$ MHCII$^{−}$ (gate 4) blood monocytes were used to illustrate GFP intensity of these subsets. E) The frequency of GFP^{+} cells among blood monocyte subsets, gates 1-5, from *Lyz2-cre*Rosa GFP^{flox} reporter mice. Each dot represents one mouse from six experiments. F) EGFP^{+} frequency within indicated populations divided by the frequency of EGFP^{+} Ly-6C^{+}MHCII^{+} (gate 2) blood monocytes in the same mouse. Blood Ly-6C$^{−}$MHCII$^{−}$ monocytes (gate 4) and pDCs were used as controls. LLN, lung-draining LN; SLN, skin-draining LN; MLN, mesenteric LN. All data are derived from 3-6 experiments. Fig. S2 accompanies this figure.

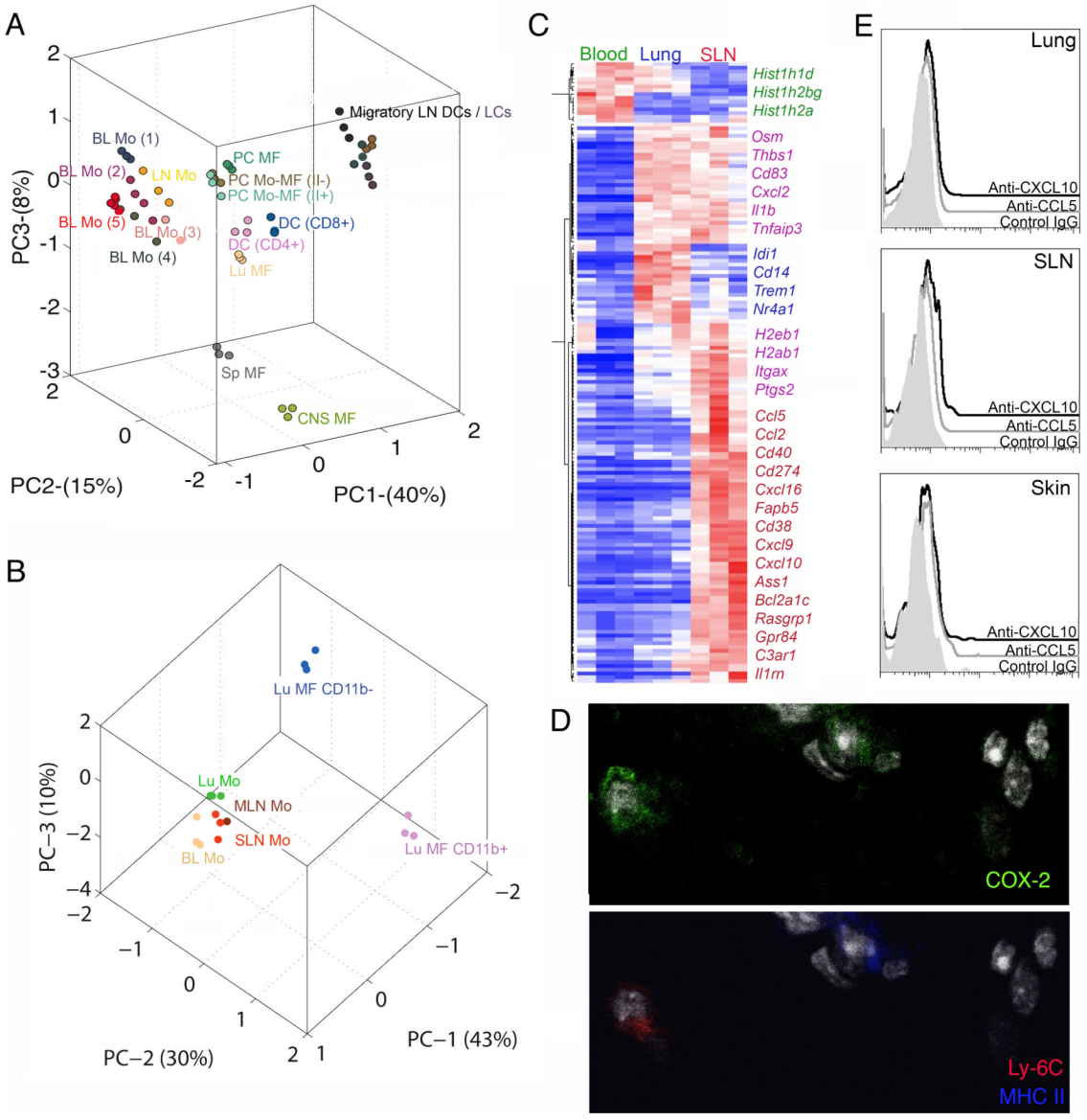

Figure 3. Gene expression analysis comparing tissue and blood monocytes with macrophages and DCs

Principle component analysis (PCA) is a mathematical procedure that depicts uncorrelated variables on each axis. Percentage shown on each axis indicate the percent of variability explained, with the first priniciple component (PC1) defined as that which explains the most variability. The placement of data in proximity indicates a closer relationship between the datasets. A) PCA of LN resident DCs $CD8^+$ and $CD4^+$, migratory LN DCs, Langerhans cells (LC), macrophages (MF), and monocytes (Mo) from LN and blood (BL) (population gates 1-5 from Fig. 2; gate numbers next to Mo symbol). PC, peritoneal cavity; CNS, central nervous system; Sp, spleen; Lu, lung. Each population is depicted with a different color. B) PCA of lung (Lu) alveolar macrophages ($CD11b^-$) and interstitial macrophages ($CD11b^+$), and monocytes from blood, lung, MLN and SLN. Each population is depicted with a different color. C) Heat map depicts genes that are elevated ≥ 3-fold in blood, lung and SLN monocytes. D) Immunostaining for COX-2 expression in $Ly6C^+$ monocytes and DCs of the lung parenchyma. E) Intracellular staining for chemokines, CXCL10 (open black) and CCL5

(open gray), along with isotype control (shaded gray) in the lung, skin and SLN. Fig. S3 and Tables S1 and S2 accompany this figure.

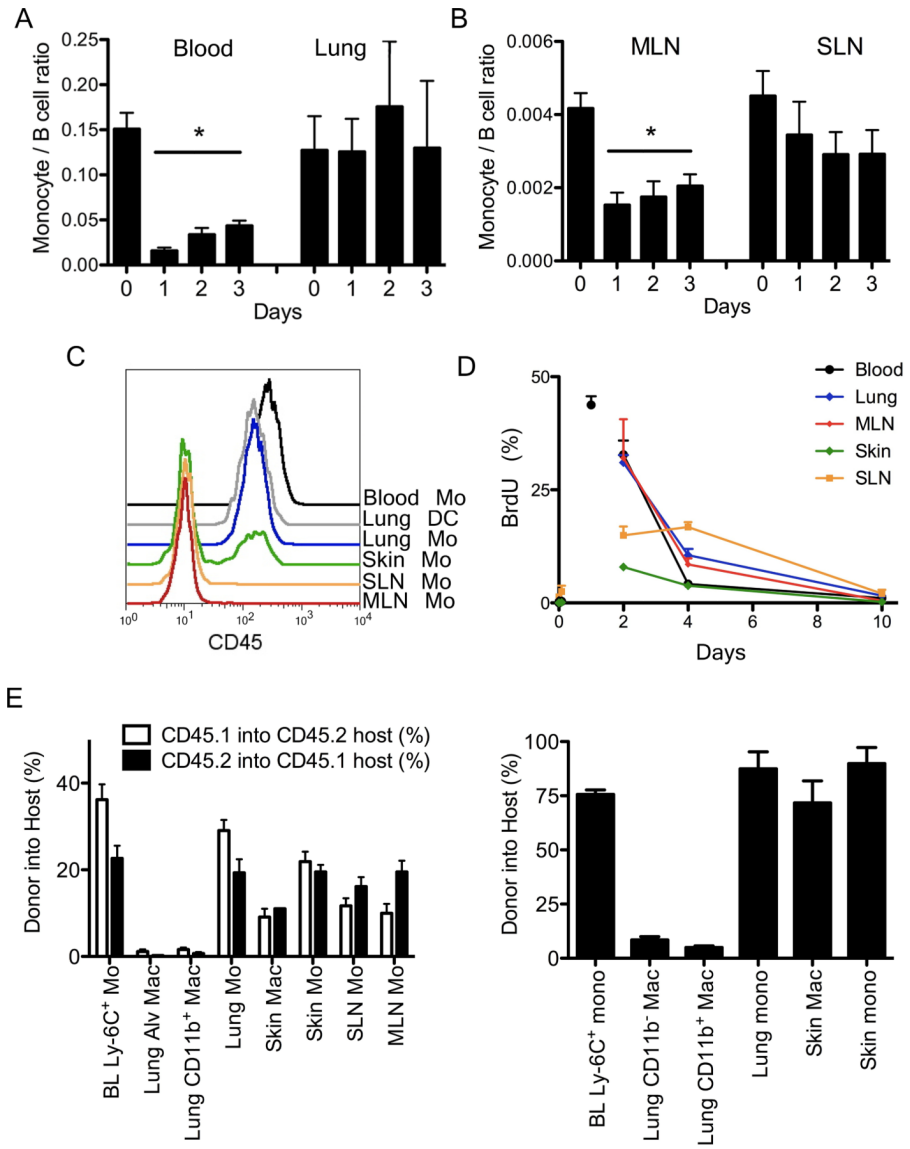

Figure 4. Turnover of tissue monocytes

Frequency of tissue monocytes, identified in tissues as in Fig. 1A, was analyzed after liposomal clodronate injection i. v. and normalized to B cells in blood and lung (A) and LNs (B). Data are representative of four experiments,2-4 mice per group. C) Overlay of lung DCs and monocytes gated from tissues after anti-CD45 was given i.v. 2 min. before euthanasia. D) BrdU pulse-chase analysis of tissue monocytes, n = 5. E) Plots depict chimerism between WT congenic parabionts at two weeks (left) and WT chimerism in *Ccr2*$^{-/-}$ hosts parabiosed with a WT partner for 1 year (right). Each bar includes 2-8 parabionts and depicts mean ± SEM. Mo,monocyte; Mac, macrophage. Fig. S4 accompanies this figure.

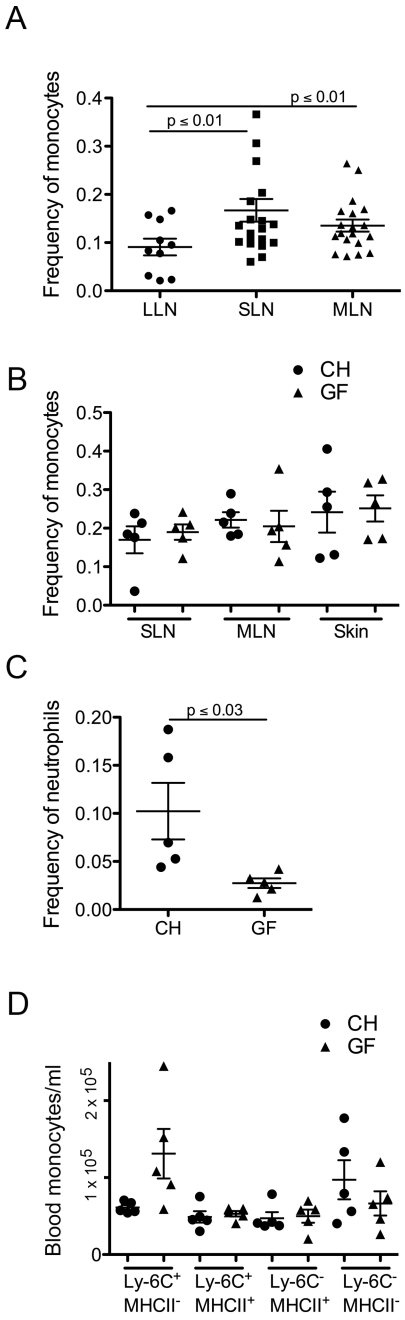

Figure 5. Commensals are not required for monocyte trafficking to tissue and LNs

A) The frequency of monocytes relative to all live cells in lung-draining (LLN), skin-draining (SLN) and mesenteric LNs (MLN) was quantified. B) Monocyte frequency in SLN and MLN of WT and germ-free mice. Monocyte (B) and neutrophil (C) frequency in skin of conventionally housed (CH) germ-free (GF) mice. D) Blood monocyte count in CH or GF mice. Each symbol, data from an individual mouse with mean ± SEM shown by bars within each dataset.

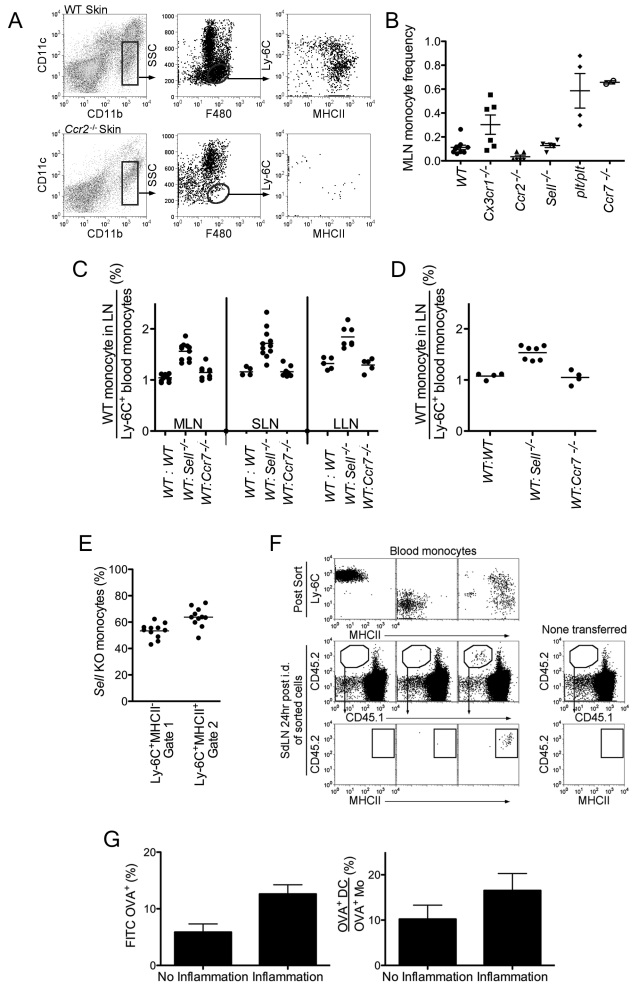

Figure 6. Tissue monocytes migrate to and from tissue to LNs via afferent lymphatics

A) Skin from WT and *Ccr2*$^{-/-}$ mice were analyzed for monocytes (gated center plots). Data are representative of two independent experiments. B) Scatter plot of MLN monocyte frequency in WT, *Cx3cr1*$^{gfp/gfp}$, *Ccr2*$^{-/-}$, *Sell*$^{-/-}$, *plt/plt* and *Ccr7*$^{-/-}$ mice. C and D) Mice were reconstituted with 1:1 mixture of CD45.1^{+} WT and CD45.2^{+} *Sell*$^{-/-}$ bone marrow (BM) cells (WT:*Sell*$^{-/-}$); CD45.1^{+} WT and CD45.2^{+} *Ccr7*$^{-/-}$ BM cells (WT:*Ccr7*$^{-/-}$); or CD45.1^{+} WT and CD45.2^{+} WT BM cells (WT:WT) as control. The frequency of LN (C) and skin (D) CD45.1 Ly-6C^{+}MHCII^{+} WT monocytes was normalized to the frequency of CD45.1 Ly-6C^{+}MHCII^{+} blood monocytes in the same mouse. E) In WT:*Sell*$^{-/-}$ chimeric mice, the frequency of blood monocyte subsets derived from *Sell*$^{-/-}$ BM cells was plotted. F) WT CD45.2^{+} blood monocytes were sorted to generate purified populations of Ly-6C^{+}MHCII^{-}, Ly-6C^{-}MHCII^{-} and Ly-6C^{-}MHCII^{+} cells (top plots). Sorted CD45.2 monocytes were adoptively transferred into the back skin of CD45.1 mice, and 24 h later, SLNs were analyzed for migration (lower plots). Representative data are shown from 3 independent experiments. G) Left, bar graph shows the frequency of OVA^{+} monocytes from total monocytes in the LLN. Right, bar graph shows the ratio of the total number of OVA^{+} DC over OVA^{+} monocytes in the LLN. Bars depict mean ± SEM. Data are representative of three independent experiments. Fig. S5 accompanies this figure.

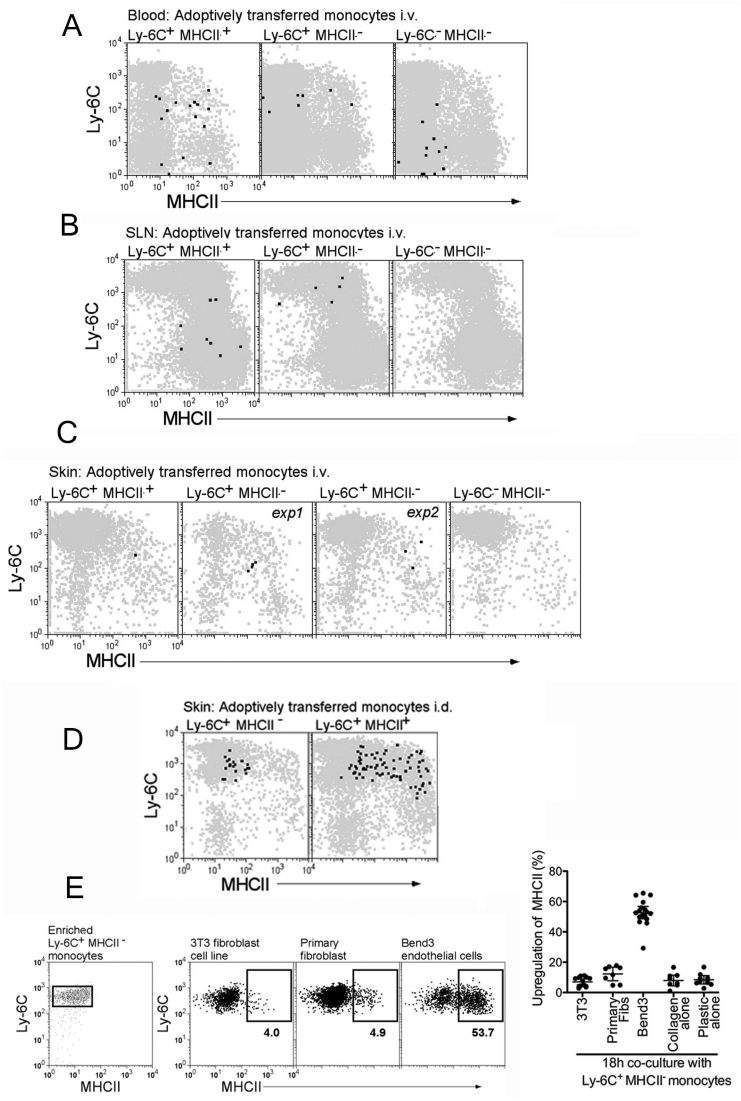

Figure 7. Conversion of Ly-6C$^+$MHCII$^-$ to Ly-6C$^+$MHCII$^+$ monocytes in vivo and in culture with endothelium

CD115$^+$GFP$^+$ blood monocyte subsets Ly-6C$^+$MHCII$^+$, Ly-6C$^+$MHCII$^-$, and Ly-6C$^-$MHCII$^-$ were sorted from CD45.2 *Cx3cr1*$^{gfp/gfp}$ mice. Sorted monocytes 1×10^6 Ly-6C$^+$MHCII$^-$, 3×10^5 Ly-6C$^+$MHCII$^+$ or 1×10^6 Ly-6C$^-$MHCII$^-$ were injected i.v. into CD45.1$^+$ WT mice, followed by i.d. injection of 2 μg LPS. At 18 h, (A) blood, (B) skin-draining LNs (SLN), and (C) skin were analyzed for monocytes migration and differentiation. Dot plot overlays display total CD11b$^+$ cells (gray) and CD45.2 GFP$^+$ adoptively transferred cells (black). C) Skin illustrates two separate experiments (exp 1, exp 2) adoptively transferring Ly-6C$^+$MHCII$^-$ monocytes. D) Purified Ly-6C$^+$MHCII$^-$ and Ly-6C$^+$MHCII$^+$ blood monocytes were injected intradermally into skin and recovered 18 h later to assess MHC II expression. E) Splenic Ly-6C$^+$MHCII$^-$ monocytes, depleted completely of MHC II$^+$ cells, were enriched by negative selection and cocultured with various cell types as shown. Ly-6C$^+$ monocytes were gated before and after the cocultures and the induction of surface MHC II was assessed and plotted (on the right). Each data point represents one experiment.